

**Polynomial dispersion of trajectories in sticky dynamics**

G. M. Zaslavsky

*Courant Institute of Mathematical Sciences, New York University, 251 Mercer Street, New York, New York 10012, USA  
and Department of Physics, New York University, 2–4 Washington Place, New York, New York 10003, USA*

M. Edelman

*Courant Institute of Mathematical Sciences, New York University, 251 Mercer Street, New York, New York 10012, USA*

(Received 10 December 2004; revised manuscript received 6 April 2005; published 8 September 2005)

Hamiltonian chaotic dynamics is, in general, not ergodic and the boundaries of the ergodic or quasiergodic area (stochastic sea, stochastic layers, stochastic webs, etc.) are sticky, i.e., trajectories can spend an arbitrarily long time in the vicinity of the boundaries with a nonexponentially small probability. Segments of trajectories imposed by the stickiness are called flights. The flights have polynomial dispersion that can lead to non-Gaussian statistics of displacements and to anomalous transport in phase space. In particular, the presence of flights influences the distribution of Poincaré recurrences. We use the distribution function of  $(l, t; \varepsilon, \varepsilon_0)$ -separation of trajectories that at time instant  $t$  and trajectory length  $l$  are separated for the first time by  $\varepsilon \ll 1$ , being initially at a distance  $\varepsilon_0 \ll \varepsilon$ . The connection of this function, called the complexity function [Afraimovich and Zaslavsky, *Chaos* **13**, 519 (2003)], with the distribution of Poincaré recurrences is established for three cases: (i) for the case of superdiffusion in standard and web maps for which the stickiness is defined by the boundaries of hierarchical sets of islands; (ii) for the case of the Sinai billiard with infinite horizon, where the stickiness is defined by zero-measure slits in the phase space; (iii) for the square billiard with a slit (bar-in-square billiard) where the Lyapunov exponent is zero and the stickiness is defined by the vicinity of the trajectory to the closest periodic trajectories obtained from the Diophantine approximation. Finally, the powerwise asymptotics of the Poincaré recurrences can be connected, in some cases, to the anomalous transport exponent.

DOI: [10.1103/PhysRevE.72.036204](https://doi.org/10.1103/PhysRevE.72.036204)

PACS number(s): 05.45.Mt, 42.50.Vk

**I. INTRODUCTION**

Typical Hamiltonian systems with low number of degrees of freedom have nonuniform phase space filled by domains of chaotic dynamics (stochastic sea, stochastic layers, stochastic webs) and domains of regular dynamics (islands, isolated periodic trajectories, etc.). All these irregularities suggest a nonuniform mixing, weak mixing, and non-Gaussian statistics of particle dynamics in phase space and, as results, anomalous transport, and particularly the appearance of infinite moments of observables. As a possible cause of all these anomalies, one can mention the existence of domains in phase space where the dispersion of trajectories is polynomial, in contrast to the exponential dispersion in Anosov type systems (for a review see [1]).

Although we cannot state at the moment that typical Hamiltonians do not have exponential dispersion at all in the infinite time limit, we can suggest that for a dense set of the values of control parameters and for sufficiently long, even astronomically long, time the dispersion of trajectories can be polynomial, i.e., the corresponding Lyapunov exponent can be zero, and the typical analysis, based on the so-called finite time Lyapunov exponents, fails. To avoid the difficulties related to the necessity of considering the  $t \rightarrow \infty$  limit, a complexity function was introduced in [2] that permits the inclusion of both cases of dispersion: polynomial and exponential. The notion of the complexity function is a generalization of the ideas of  $\varepsilon$ -separation in phase space [3–5]. The generalization consists of a new probability distribution function of the first  $(l, t; \varepsilon, \varepsilon_0)$ -separation of a pair of trajec-

tories, initially at a distance  $\varepsilon_0$ , and finally at time  $t$  at a distance  $\varepsilon$ ,  $\varepsilon_0 \ll \varepsilon \ll 1$ , and with the length of the trajectories  $\sim l$ . Thus, one can consider in a natural way any instability of trajectories in phase space. The goal of this paper is to connect the complexity function, as the characteristic of the trajectory dispersion, to some observables such as the Poincaré recurrence distribution or the evolution of moments of the particle displacements, i.e., particle transport.

We will demonstrate such connection for three types of systems.

(i) For standard and web maps. There exist an infinite number of values of a control parameter  $K$  such that trajectories are sticky to the islands' boundaries and the transport is superdiffusive.

(ii) For the Sinai billiard with infinite horizon. This system has positive Lyapunov exponent and zero-measure domains in the phase space, which are isolated from the domain of ergodic and stochastic motion. Nevertheless, these zero-measure domains induce anomalous superdiffusive transport [1].

(iii) For the billiard square-with-slit (bar inside) or for the billiard square-in-square [6,7]. The Lyapunov exponent is zero for these billiards and the stickiness can be interpreted as the trajectory vicinity to different parts of the periodic trajectories.

It is worthwhile to note that in some cases the powerwise distribution of Poincaré recurrences can be connected to the transport exponents (see more in the review [1]) and, in this way, the complexity function can be related to the transport and diffusion.

## II. COMPLEXITY FUNCTION: DEFINITION

The complexity function (CF) was introduced in [2] in order to describe systems with different types and level of instability in phase space. Referring to a very general concept of statistical physics, one can introduce the complexity  $C$  of a system as the number  $N$  of possible, in some sense equivalent, states of the system that we cannot distinguish. Then  $C=N$  measures the “phase volume” of the system due to the existence of a level of indefiniteness, and the value  $S=\ln C=\ln N$  measures the entropy of the system.

The notion of complexity can be developed for systems with chaotic dynamics where the indefiniteness appears as a result of the local instability of trajectories in the system’s phase space. Instability leads to the separation of trajectories that were initially close to each other in time. Let  $\delta$  be the level of resolution, or coarse graining, in phase space, i.e., two points with a distance  $d_0 < \delta$  are not distinguishable. Two initially close trajectories with the initial distance  $d_0 \ll \delta$  will not be separated at any time  $t$ , i.e.,  $d(t) < \delta$ , if the dynamics is stable, and they will be separated at some  $t$ ,  $d(t) \geq \delta$ , if the dynamics is unstable. Thus a bunch of trajectories that starts within an interval  $\delta$  reveals a number of  $\delta$ -distinguishable trajectories after some time, and that is the mechanism of growth of  $C=N(t)$ .

The first implementation of this concept for a dynamical system with chaos was by Bowen [5] who introduced the notion of  $(\varepsilon, n)$ -complexity. Let  $d(n)$  be the distance between two trajectories at discretized time  $t=n$ . Two trajectories, according to [5], are  $(\varepsilon, n)$ -separated if there exists such  $n_1 \in (0, n)$  that  $d(n_1) \geq \varepsilon$ . Then the maximal number of  $(\varepsilon, n)$ -separated trajectories that started at the phase space domain  $A$  is the  $(\varepsilon, n)$ -complexity  $C(\varepsilon, n; A)$  of the domain  $A$ . In particular, it was shown in [5] that for  $A$ -axiom systems

$$\lim_{\varepsilon \rightarrow 0} \overline{\lim}_{n \rightarrow \infty} \frac{1}{n} \ln C(\varepsilon, n; A) = h_{\text{top}}(A) \quad (1)$$

where  $h_{\text{top}}$  is the topological entropy. The result (1) can be easily understood if the phase space is uniformly and exponentially unstable, i.e., for any two trajectories in  $A$ ,

$$d(n) = d(0) \exp(hn), \quad h = h_{\text{top}}. \quad (2)$$

Although the introduction of the  $(\varepsilon, n)$ -complexity was important to study chaotic dynamics, it appears to be impossible to apply it to realistic Hamiltonian systems. Here are some reasons for that.

(i) Real Hamiltonian chaos does not have uniform characteristics of the instability of trajectories in phase space and different arbitrarily large and arbitrarily long segments of trajectories have different increments and even different types of separation.

(ii) Although the introduced complexity  $C(\varepsilon, n; A)$  depends on time  $n$ , this dependence disappears in Eq. (1) after the limit  $n \rightarrow \infty$  that may not exist in a strong sense.

(iii) The definition of  $(\varepsilon, n)$ -separation includes an arbitrary time instant  $n_1 \in (0, n)$ . This definition leaves some in-

definiteness about the trajectories during the time interval  $(n_1, n)$ . This interval can be arbitrarily long for the case of polynomial dependence of  $C(\varepsilon, n; A)$  on  $n$ .

(iv) Definition (1) cannot be applied to a system with polynomial dispersion of trajectories or to systems with pseudochaotic dynamics ( $h=0$  but the dynamics is random) (for more discussions, see [1]).

The typical and most often used way to study nonuniform chaotic dynamics is to consider the distribution function  $\rho(\sigma)$  of the finite time Lyapunov exponent  $\sigma$  [8,9]

$$\sigma_{\Delta t} = \frac{1}{\Delta t} \ln[d(t)/d(0)]. \quad (3)$$

Different simulations show that in the Hamiltonian dynamics  $\rho(\sigma_{\Delta t})$  possesses a “central peak,” i.e., there exists a local maximum of  $\rho(\sigma_{\Delta t})$  near the value  $\sigma_{\Delta t}=0$  [10] (see more discussion in [11]). This maximum appears due to sticky domains in phase space that cannot be characterized by the exponential dispersion of trajectories.

The complexity function of [2] was proposed to avoid the described difficulties (i)–(iv) and to provide a more adequate description of sticky chaotic and pseudochaotic dynamics. The main feature of the CF is to consider small but finite dispersion of a pair of trajectories by the distance  $\varepsilon$ ,

$$\varepsilon_0 \ll \varepsilon \ll 1, \quad (4)$$

with initial dimensionless distance  $\varepsilon_0$  and the characteristic size of the phase space of order 1. Consider again a small domain  $A$  of diameter  $d_A$  and a set  $M_A(N, \varepsilon_0)$  of a large number  $N$  of pairs of trajectories such that in each pair the distances between initial points within each pair are  $\varepsilon_0$ . In the case of

$$\varepsilon_0 < d_A \ll \varepsilon \quad (5)$$

all trajectories are  $\varepsilon$ -indistinguishable, i.e., for a fairly small observation time an observer sees only one trajectory. As time advances, more and more pairs appear to be  $\varepsilon$ -distinguishable. Let  $N_A(l, t; \varepsilon, \varepsilon_0)$  be the number of  $\varepsilon$ -distinguishable pairs such that (i) all pairs have initial distance  $\varepsilon_0$  at  $t=0$ ; (ii) all pairs of  $N_A(l, t; \varepsilon, \varepsilon_0)$  are  $\varepsilon$ -separated for the first time at  $t$  within a small interval  $dt$ ; (iii) all pairs of  $N_A(l, t; \varepsilon, \varepsilon_0)$  have the length of trajectories  $l$  (up to small corrections of the order  $\varepsilon$ ) with

$$l = \int_0^t e^0(t') dl(t') \quad (6)$$

where  $e^0(t)$  is the unit vector along the trajectory and  $dl(t)$  is a directed element of the trajectory in phase space.

Following [2], the CF  $C_A(l, t; \varepsilon, \varepsilon_0)$  is defined as

$$C_A(l, t; \varepsilon, \varepsilon_0) = N_A(l, t; \varepsilon, \varepsilon_0). \quad (7)$$

The main differences of this consideration, compared to the definition of  $C(\varepsilon, n; A)$  in [5], are the following: (i) the CF is defined for an arbitrary (discrete or continuous) time; (ii) the time  $t$  in the CF is the time of the first  $\varepsilon$ -separation of pairs while the instant  $t_1$  of separation in [5] can be any  $t_1 \in (0, t)$ ; (iii) since trajectories in phase space have fairly

complicated shapes, there are many paths of  $\varepsilon$ -separation at time instant  $t$ , and different paths can be of very different lengths  $l$  for the same  $t$ ; this difference cannot be discerned by  $C(\varepsilon, n; A)$ .

The definition (7) can be easily modified for maps with discrete time. Let  $\{t_0, t_1, \dots, t_k, \dots\}$  be a sequence of time instants for the Poincaré map of the system. We assume that such a map exists and the intervals  $t_{n+1} - t_n$  may not be equal. Let  $n$  be such a step number that for  $k \leq n - 1$  a pair of trajectories is not  $\varepsilon$ -separated, and for  $k = n$  the distance between particles of the pair is  $\geq \varepsilon$ . Any trajectory in phase space  $(p, q)$  is defined as the sequence  $\{p_0, q_0; p_1, q_1; \dots; p_n, q_n\}$  of the values  $(p_k, q_k)$  at time  $t_k$ . Then the length of a trajectory at time instant  $t_n$  is

$$l_n = \sum_{k=1}^n |\Delta l_k|, \quad (\Delta l_k)^2 = (\Delta p_k)^2 + (\Delta q_k)^2, \quad \Delta p_k = p_k - p_{k-1}, \quad \Delta q_k = q_k - q_{k-1}. \quad (8)$$

A typical situation, for example, for the standard map is the case when a diffusion of chaotic trajectories is considered in a cylinder phase space  $p \in (-\infty, \infty)$ ,  $q \in (0, 2\pi)$ . Then for larger  $n$  trajectories are fairly far from the origin but, nevertheless, the value of  $\Delta l_k$  depends strongly on  $\Delta q_k$ . A pair is considered to be  $(l_n, t_n; \varepsilon, \varepsilon_0)$ -separated, if, for a pair initially separated by  $\varepsilon_0 \ll \varepsilon$ , the first  $\varepsilon$ -separation of the pair appears at time instant  $t_n$ , where  $l_n$  is the length (8) of a trajectory in the pair and the difference between lengths of trajectories in the pair is neglected due to the small  $\varepsilon \ll 1$ . Again, let us mention a difference between this definition and that of [5] where  $l_n$  was not introduced and  $\varepsilon$ -separation could appear at any  $k < n$ . The corresponding definition of the complexity function is similar to Eq. (7):

$$C_A(l_n, t_n; \varepsilon, \varepsilon_0) = N_A(l_n, t_n; \varepsilon, \varepsilon_0), \quad (9)$$

where  $N_A(l_n, t_n; \varepsilon, \varepsilon_0)$  is the number of  $\varepsilon$ -distinguishable pairs with length  $l_n \in (l_n, l_n + dl)$  and separation time  $t_n$ . In the following we will consider the asymptotics of  $t \rightarrow \infty (n \rightarrow \infty)$  and the difference between Eqs. (7) and (9) is negligible.

Although the CF is defined with respect to the domain  $A$ , the definitions (7) and (9) are not quite local and, in fact, they can be considered as semilocal since for large  $t$  trajectories can depart fairly far from  $A$  in phase space.

### III. COMPLEXITY FUNCTION IN WORK

In practice, definition (9) is not sufficient and not convenient enough since it is not global and some limits like  $\varepsilon \rightarrow 0$  or  $N \rightarrow \infty$  cannot be performed and a finite  $\varepsilon_0$  and  $N$  should be specified relative to the problem. Let us associate with a domain  $A$  a density  $\rho_A(l, t; \varepsilon, \varepsilon_0)$ , i.e., the normalized density of pairs, taken in the domain  $A$ , initially at the distance  $\varepsilon_0$ , and  $\varepsilon$ -separated for the first time at the time instant  $t$  within the interval  $dt$  and with the natural length of the trajectory  $l$  within the interval  $dl$ . We assume bounded dynamics with the normalization conditions

$$\int_0^\infty dl dt \rho_A(l, t; \varepsilon, \varepsilon_0) = 1. \quad (10)$$

For simplicity, we can also assume a limited uniformity in phase space, i.e.,  $\rho_A$  does not depend on the choice of the ensemble of initial pairs, and a limited uniformity of the increment of instability, i.e.,  $\rho_A$  depends on the value  $\varepsilon/\varepsilon_0$  under condition (4) rather than on  $\varepsilon$  and  $\varepsilon_0$  separately. If  $N$  is the number of initially considered pairs of trajectories in domain  $A$ , then

$$c_{A,N}(l, t; \varepsilon, \varepsilon_0) \equiv N_{A,N}(l, t; \varepsilon, \varepsilon_0)/N = C_{A,N}(l, t; \varepsilon, \varepsilon_0)/N \quad (11)$$

is the normalized complexity function if  $N$  is sufficiently large. The last equality in (11) emphasizes that the non-normalized complexity function is simply a number of  $(\varepsilon, l, t)$ -dispersed pairs, which is convenient for numerical calculations. Now the CF density  $\rho_A(l, t; \varepsilon, \varepsilon_0)$  can be defined as in [2]:

$$\rho_{A,N}(l, t; \varepsilon, \varepsilon_0) dl dt = [c_{A,N}(l + dl, t + dt; \varepsilon, \varepsilon_0) - c_{A,N}(l, t; \varepsilon, \varepsilon_0)] dl dt > 0 \quad (12)$$

since  $c_{A,N}$  is a nondecreasing function.

It is worthwhile to mention the kind of limits applied to Eq. (11) and those that are not. For finite  $N$ , the CF  $C_{A,N}(l, t; \varepsilon, \varepsilon_0)$  reaches the maximum value  $\max C_{A,N}$  at some  $t_{\max}$ , if  $\varepsilon$  and  $\varepsilon_0$  are fixed. That means that the definition of  $\rho_{A,N}$  has the corresponding constraints for finite  $N$ . We suggest that the normalized CF  $c_A(l, t; \varepsilon, \varepsilon_0)$  appears in the limit

$$c_A(l, t; \varepsilon, \varepsilon_0) = \lim_{N \rightarrow \infty} \frac{1}{N} C_{A,N}(l, t; \varepsilon, \varepsilon_0) \quad (13)$$

but the time  $t$  is finite at the instant of first  $\varepsilon$ -separation with  $\varepsilon \ll 1$ . This condition is different from that usually considered in the definitions of Lyapunov exponent, Kolmogorov-Sinai entropy, and topological entropy. It is also different from the Bowen definition of  $(\varepsilon, n)$ -separation, where the discrete time  $n$  can be arbitrarily large compared to the time instant  $n_0$  of the first  $\varepsilon$ -separation of trajectories.

The local complexity function can provide fairly detailed information about the quasilocal phase space dynamics, but it is most appropriate to introduce some global characteristics. It is convenient to use

$$C(l, t; \varepsilon, \varepsilon_0) = \sum_{A \subset \Gamma} C_A(l, t; \varepsilon, \varepsilon_0) m(A)/m(\Gamma) \quad (14)$$

as the global CF, where the full phase space of ergodic or quasiergodic dynamics is

$$\Gamma = \cup A. \quad (15)$$

and  $m(A)$  and  $m(\Gamma)$  are measures of  $A$  and  $\Gamma$ . The corresponding global complexity density is

$$\rho(l, t; \varepsilon, \varepsilon_0) = \lim_{N \rightarrow \infty} \frac{1}{m(\Gamma)} \sum_{A \subset \Gamma} m(A) \rho_{A,N}(l, t; \varepsilon, \varepsilon_0) \quad (16)$$

as a generalization of Eq. (13).

It is sufficiently easy to calculate  $\rho(l, t; \varepsilon, \varepsilon_0)$  numerically but, as a compensation for this simplification, it is not so trivial to connect  $\rho(l, t; \varepsilon, \varepsilon_0)$  with the observables related to kinetics and transport. For example, in the important case of self-similar kinetics

$$\rho(l, t; \varepsilon, \varepsilon_0) dl dt = t^{\mu_r/2} \rho(\xi, t; \varepsilon, \varepsilon_0) dt d\xi \quad (17)$$

where

$$\xi = ll^{\mu_r/2} \quad (18)$$

and the exponent  $\mu_r$  is not identified yet. In the case of the exponential and uniform dispersion of trajectories [2]

$$\rho(l, t; \varepsilon, \varepsilon_0) = (\text{const}) \times (\varepsilon/\varepsilon_0)^{\tilde{d}} e^{ht} \rho_l \quad (19)$$

where  $\tilde{d}$  is the phase space dimension and  $h$ , for the models considered below with  $1\frac{1}{2}$  or 2 degrees of freedom, is the topological entropy (in many physical problems with chaotic dynamics and mixed phase space,  $h$  is of the same order as the Kolmogorov-Sinai entropy or the Lyapunov exponent averaged over different  $A$  [9]), and  $\rho_l$  represents the part that depends on  $l$ . In the simplest situation  $\rho_l = \delta(l - l(t))$ , i.e., it does not depend on the initial point.

The formula (19) appears in the case of exponential dispersion of pairs when the distance between two trajectories  $d(t) = d(0)\exp(ht)$  is similar to (2). The number of pairs in  $A$ , in the case of uniform mixing, is proportional to the volume of  $A$ , i.e., for  $d(0) = \varepsilon_0$ ,  $d(t) = \varepsilon$ , the complexity density should be proportional to  $(\varepsilon/\varepsilon_0)^{\tilde{d}}$  with  $\tilde{d}$  as the box dimension of  $A$ . Although the expression (19) can be useful for some cases, it is not generic and our simulations in Sec. IV show a deviation from the exponential dispersion of trajectories.

Our next goal is to find a link between  $\rho$  and other observables or, more specifically, between  $\rho$  and the Poincaré recurrence distribution  $P(t; A)$ ,

$$\int_0^\infty P(t; A) dt = 1, \quad (20)$$

and between  $\rho$  and the distribution function of displacement  $F(x, t)$ , i.e., the probability density to be at point  $x$  at time  $t$ . The Poincaré recurrences to the domain  $A$  are defined through the set  $\{t_1, t_2, \dots\}_{rec}$  where  $t_k$  is the time instant of the  $k$ th escape from  $A$  of a trajectory initially at  $t_0$  in  $A$ . The intervals  $\Delta t_k = t_{k+1} - t_k$  are called Poincaré cycles, i.e., the time between two successive escapes of the trajectory from  $A$ . For large  $T$  the number of Poincaré cycles  $N_{rec}(T, A)$  is large and  $P(t; A) dt \sim n_{rec}(t, A) / N_{rec}(T, A)$  where  $n_{rec}$  is the number of cycles of length  $t \in (t, t+dt)$ . If  $t \ll T$  and  $t \rightarrow \infty$ , the difference between the discrete time dependence of  $n_{rec}$  and the continuous one is negligible (see [12]).

Assume also that the dynamics is topologically transitive, i.e., if  $x$  is a point in a part of the phase space with chaotic dynamics (called the stochastic sea) then the considered trajectories can be arbitrarily close to  $x$  when  $t \rightarrow \infty$  [13]. Then there is the following conjecture.

*Conjecture 1.* Let the full phase space of dynamics  $A_\Gamma$  with  $\Gamma < \infty$  have only the singular domain  $A_S \subset A_\Gamma$  and let the

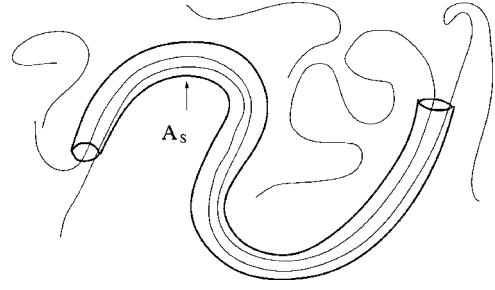


FIG. 1. An example of two trajectories in a sticky domain  $A_S$ .

dynamics be area preserving and uniform in  $A_\Gamma \setminus A_S$ . We also assume that such a splitting of  $A_\Gamma$  into two domains  $A_S$  and  $A_\Gamma \setminus A_S$  is possible or it is a fairly good approximation. The singular domain  $A_S$  is a sticky domain or quasitrap where trajectories can spend an arbitrarily long time before their escapes (see Fig. 1), and the probability of a long stay in  $A_S$  is not exponentially small. Then for  $A \subset A_\Gamma$  and  $A \cap A_S = \emptyset$  we have asymptotically

$$P(t; A) \sim \int_0^\infty dl \rho_{A_S}(l, t; \varepsilon, \varepsilon_0), \quad t \rightarrow \infty. \quad (21)$$

The result (21) follows from the property that the mixing in  $A_S$  is much slower than in any  $A \subset A_\Gamma$ . If the escape probability

$$P_{esc}(t) \sim (\text{const})/t^{\gamma_{esc}}, \quad t \rightarrow \infty, \quad (22)$$

then [1] for  $A \cap A_S = \emptyset$

$$P(t; A) \sim (\text{const})/t^\gamma, \quad t \rightarrow \infty, \quad (23)$$

with

$$\gamma = \gamma_{esc}. \quad (24)$$

This result can be understood in the following way. Consider arbitrary  $A$  not too close to  $A_S$  and a set of well mixed trajectories that do not enter  $A_S$  during time  $t$ . For these trajectories

$$P(t; A) \sim m(A) \exp[(-\text{const}) \times t] \quad (25)$$

where  $\text{const} \sim h_{\text{top}}(A)$  [1, 14, 15]. When  $t \rightarrow \infty$ , the probability density (25) decays exponentially. Nevertheless, due to the topological transitivity, there exists a finite probability for trajectories to enter  $A_S$  and escape from  $A_S$  following the rule (22). Then we can write simply

$$P(t; A) = P_1(t; A) + P_2(t; A) \quad (26)$$

where  $P_1(t; A)$  is related to the trajectories that did not enter  $A_S$  during time  $t$  and  $P_2(t; A) \neq 0$  is related to the trajectories that enter  $A_S$  at least once during the time  $t$ . As  $t \rightarrow \infty$  the first term in (26) disappears and for the second one we have

$$P(t; A) \sim P(t; A_S), \quad t \rightarrow \infty, \quad (27)$$

which leads to (24). This statement was never proved but it was supported by many numerical observations (see references in [1]).



Similar arguments can be applied to the conjecture (21). Indeed, the long time recurrences can appear with a reasonable not exponentially small probability after trajectories' entrance into the singular domain  $A_S$  and their following escape. Correspondingly, long time separation of a pair appears only when the initial conditions of the pair belong to  $A_S$ . We consider one trajectory as the reference one and a second trajectory very close to the reference one. When the separation becomes  $\varepsilon$ , we start a new pair with the same reference trajectory and a new second trajectory, and so on (see [10] where the procedure is described in detail). The reference trajectory of the pairs is visiting different parts of the phase space and, due to the topological transitivity, enters the singular domain  $A_S$  (see Fig. 1).

The dynamics, which is random in some sense but has zero Lyapunov exponent, is called pseudochaotic. Different examples of pseudochaos are considered in [1,6,7], and, particularly, the dynamics in polygonal billiards is pseudochaotic. For pseudochaotic dynamics, it can happen that there is a global uniformity of phase space and there is no special singular domain  $A_S$ . Then, instead of (21), there is a stronger relation

$$P(t;A) = P(t) \sim \int_0^\infty dl \rho(l,t;\varepsilon,\varepsilon_0), \quad t \rightarrow \infty, \quad (28)$$

i.e., no dependence on the domain  $A$ . In the next section we provide four examples to illustrate (24) and (28).

In some examples of the following sections we consider discrete maps instead of continuous flows. In these cases the time variable is discrete,  $t_n = n$ , and instead of  $P(t)$  we will consider  $P(t_n) = P(n)$ . This is valid for the cases when the time interval between the consecutive steps of the map is constant.

#### IV. EXAMPLES FOR THE STANDARD MAP AND WEB MAP

The standard map is defined as

$$p_{n+1} = p_n - K \sin x_n, \quad x_{n+1} = x_n + p_{n+1} \quad (29)$$

on the torus  $(p, x) \in (-\pi, \pi)$ . It was shown in [16] that there exists a set of special values of  $K_l^*$  such that the distribution of recurrences  $P(t)$  has power tails for  $t \rightarrow \infty$  due to stickiness to the islands of the so-called accelerator mode. Examples of such values of  $K_l^*$  were presented in [17–19]. The set  $K_l^*$  seems to be as dense as rationals, but for some values of  $K_l^*$  the effect of stickiness is much stronger than for others. One such value is  $K^* = 6.908\,745$  [17].

The setup for simulations is the following. Consider a reference trajectory  $z_k(t) = (x_k(t), p_k(t))$  with initial condition  $(x_k(0), p_k(0)) \in A$  and a corresponding pairing trajectory  $z_k^{(1)}(t) = (x_k^{(1)}(t), p_k^{(1)}(t))$  with initial condition  $(x_k^{(1)}(0), p_k^{(1)}(0)) \in A$  such that

$$\text{dist}\|z_k^{(1)}(0) - z_k(0)\| = \varepsilon_0 \ll \varepsilon \ll 1. \quad (30)$$

After some time interval  $t_1$  the pairing trajectory crosses a tube of radius  $\varepsilon$  around the reference trajectory (see Fig. 2).

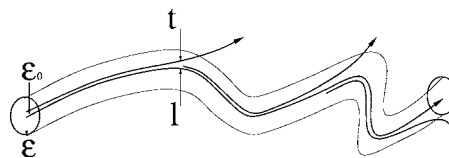


FIG. 2. Exit of pairing trajectories from the  $\varepsilon$ -tube around a reference trajectory.

The length of the tube at that moment is  $l_1$ . Then another pairing trajectory  $z_k^{(2)}(t) = (x_k^{(2)}(t), p_k^{(2)}(t))$  is started with  $\text{dist}\|z_k^{(2)}(t_1) - z_k(t_1)\| = \varepsilon_0$ . It crosses the tube for the first time at time instant  $t'_2 = t_1 + t_2$  and the tube length  $l'_2 = l_1 + l_2$ . This procedure can be applied many times for the same reference trajectory  $z_k$ , and for a set  $\{z_k\}$ ,  $z_k \in A$ , of reference trajectories. As a result, we obtain  $N(l,t;\varepsilon,\varepsilon_0)$  events of  $(l,t,\varepsilon)$ -separation, i.e., the number of pairs that are separated by  $\varepsilon$  after time  $t$  and length  $l$ . It is the complexity function that can be normalized as [2]

$$\rho(l,t;\varepsilon,\varepsilon_0) = N(l,t;\varepsilon,\varepsilon_0)/N_0 \quad (31)$$

where  $N_0$  is the full number of separated pairs that includes separation with any  $t$  and  $l$ .

Simulation gives the power laws (23) with  $\gamma = 3.3 \pm 0.1$  for  $K^* = 6.908\,745$  and  $\gamma = 3.1 \pm 0.1$  for  $K = 6.1$  (see Fig. 3). The first value is in good agreement with the previous result  $\gamma = 3.25 \pm 0.1$  [16]. The second result can be interpreted as the result for separation of orbits in the case of “normal” diffusion. Consider an enveloped, or coarse-grained, phase volume  $\bar{\Gamma}(t)$  and estimate how it grows with time. If diffusion is normal for the standard map, then  $\Delta p \equiv \langle |p|^2 \rangle^{1/2} \sim t^{1/2}$  and  $\Delta x \sim t \Delta p \sim t^{3/2}$ . In this case the growth of an enveloped phase volume  $\bar{\Gamma}$  is

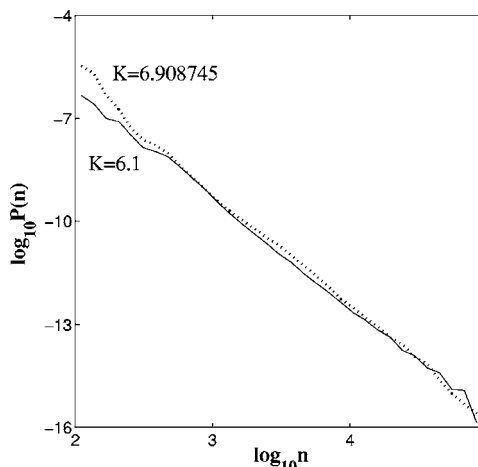


FIG. 3. Probability density of recurrences after  $n$  steps,  $P(n)$ , for the standard map:  $5 \times 10^7$  iterations for 77 824 pairs of trajectories. Initial conditions are taken from a box  $2.5 < x < 3$ ,  $0.21 < p < 0.22$ . Initial separation of a pair  $\varepsilon_0 = 10^{-6}$  along the  $p$  axis;  $\varepsilon = 0.01$ . For  $K = 6.1$  the slope is  $-3.1$  in the time interval  $(2 < \log_{10} n < 5)$ ; for  $K = 6.908\,745$  the slope is  $-3.3$  for the time interval  $(3 < \log_{10} n < 5)$ .

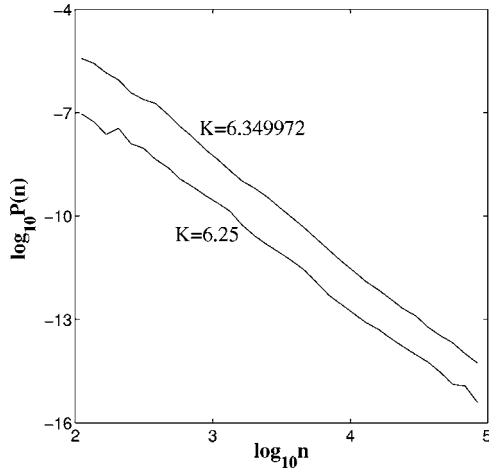


FIG. 4. Probability density of recurrences after  $n$  steps,  $P(n)$ , for the web map:  $5 \times 10^7$  iterations for 81 920 pairs of trajectories. Initial conditions are taken from a box  $2.5 < x < 3$ ,  $0.21 < p < 0.22$ . Initial separation of a pair is  $\varepsilon_0 = 10^{-6}$  along the  $v$  axis;  $\varepsilon = 0.01$ . For  $K=6.25$  the slope is  $-2.9$  in the time interval ( $3.2 < \log_{10} n < 4.5$ ); for  $K=6.349972$  the slope is  $-3.2$  for the time interval ( $3.3 < \log_{10} n < 4.9$ ).

$$\bar{\Gamma}(t) = \overline{\Delta p(t) \Delta x(t)} = (\text{const}) \times t^{1/2} t^{3/2} = (\text{const}) \times t^2. \quad (32)$$

From Eq. (32) the probability of return to an initial small phase volume  $\Gamma_0$  during the time interval  $(0, t)$  is

$$P_{int}(t) \sim \Gamma_0 \bar{\Gamma}(t) = (\text{const})/t^2, \quad (33)$$

where  $P_{int}(t)$  is the integrated probability  $P(t)$ , i.e., the probability density of recurrences is

$$P(t) = -dP_{int}(t)/dt = (\text{const})/t^3. \quad (34)$$

It is worthwhile to mention that the value  $\gamma=3$ , as follows from Eq. (34) for the normal diffusion, coincides with the same value of  $\gamma$  for some cases of anomalous diffusion (see for example the case of the Sinai billiard in Sec. V). First, the values of  $\gamma$  for the anomalous cases were never rigorously evaluated, i.e., small deviations from  $\gamma=3$  and from the power law are possible (for example,  $\log t$  terms could appear in the Sinai billiard model). Second, the power law behavior for the Poincaré recurrences does not imply anomalous transport since the latter needs a specific deviation from the Gaussian distribution. A small deviation of  $\gamma=3.1$  from this value can be explained by a remnant stickiness or by errors of simulation.

Similar results are obtained for the web map of fourfold symmetry:

$$u_{n+1} = v_n, \quad v_{n+1} = -(u_n + K \sin v_n). \quad (35)$$

The values of  $K$  were taken as  $K^* = 6.349972$  that generates strong stickiness [16] and  $K=6.25$  for which the influence of stickiness is almost negligible for the considered time. The corresponding results for  $\gamma$  are almost the same:  $\gamma = 3.2 \pm 0.1$  for  $K^*$  and  $\gamma = 2.9 \pm 0.1$  for  $K=6.25$  (see Fig. 4). These results support Conjecture 1.

The domains  $A$  for both examples were chosen in the most uniform area of the stochastic sea, i.e., fairly far from the main sticky islands observed in [17–19]. The results should not depend on the choice of  $A$  if  $A \cap A_S = \emptyset$ . In fact the singular area  $A_S$  is not strictly localized and the assumption of  $A \cap A_S = \emptyset$  is a kind of approximation that can be good for specific values of  $K^*$  as it was mentioned in [17–19].

## V. SINAI BILLIARD

The Sinai billiard is a well known object of dynamics but some questions related to transport are still waiting for solutions [1,20] due to the existence of long-lasting flights (see Fig. 5 for a trajectory in the periodically continued billiard known as the Lorentz gas). In Fig. 6 we show the distribution of Poincaré recurrences  $P(t)$  for the Sinai billiard with trajectories on the torus  $(x, y) \in (-1, 1; -1, 1)$ . The beginning of the curve corresponds to the result (25), i.e., to the exponential decay of the distribution of recurrences, but the large time asymptotics provides a power tail dependence (23) with  $\gamma=3$ . The inset in Fig. 6 shows the exponential decay of  $P(t)$  for small enough time, and then a crossover to the power law. The point of crossover depends on the size of the domain  $A$  to return, but the general type of the curve does not depend on the location of  $A$ .

In Fig. 7 we show the distribution of the number of pairs  $N(t)$  that are  $\varepsilon$ -separated for the first time at  $t$ . The curve shows the crossover from exponential to power decay with the same  $\gamma=3$ , in correspondence with Conjecture 1.

## VI. PSEUDOCHAOTIC BILLIARD

We consider a bar-in-square (slit-in-square) billiard and the Lorentz gas analog for it (see Fig. 8). It has zero Lyapunov exponent and the trajectories with irrational tangent have weak mixing and randomness (see the corresponding references in [21,6,1], where the results for the kinetics of particles are presented).

Due to the conservation of velocity along the horizontal axis  $x$ , the diffusion process is only along  $y$ . The trajectory is called irrational if  $\tan \vartheta$  is irrational and  $\vartheta$  is the angle with the  $x$  axis. Only irrational trajectories perform the diffusion. There are no islands in the phase space and there is no fast mixing process since the Lyapunov exponent is zero. The mixing is due to diffusion. It was shown by simulation in [6] that

$$\gamma \approx 2.75, \quad \mu \approx 1.75, \quad (36)$$

where  $\mu$  is the so-called transport exponent:

$$\langle |y| \rangle = \int_{-\infty}^{\infty} dy |y| F(y, t) = (\text{const}) \times t^{\mu/2}, \quad t \rightarrow \infty, \quad (37)$$

and  $F(y, t)$  is the distribution function (probability density) to find a particle at coordinate  $y$  at time interval  $(t, t+dt)$  for an ensemble of a large number of trajectories with different irrational  $\tan \vartheta$ .

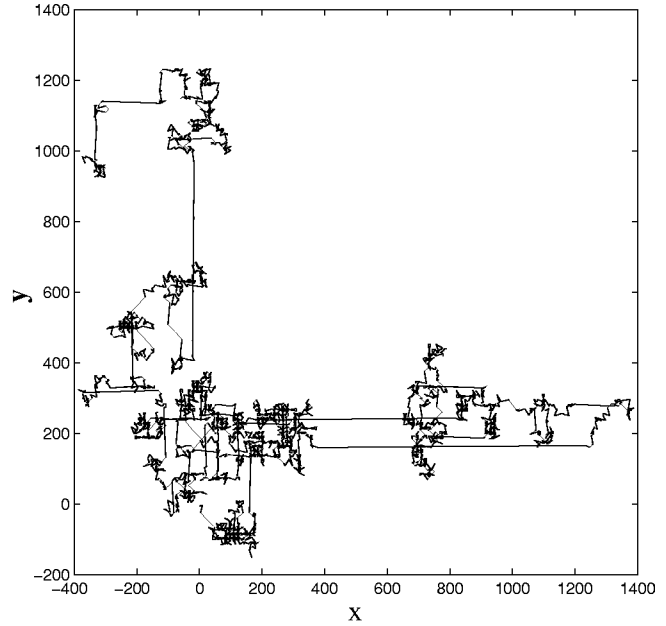
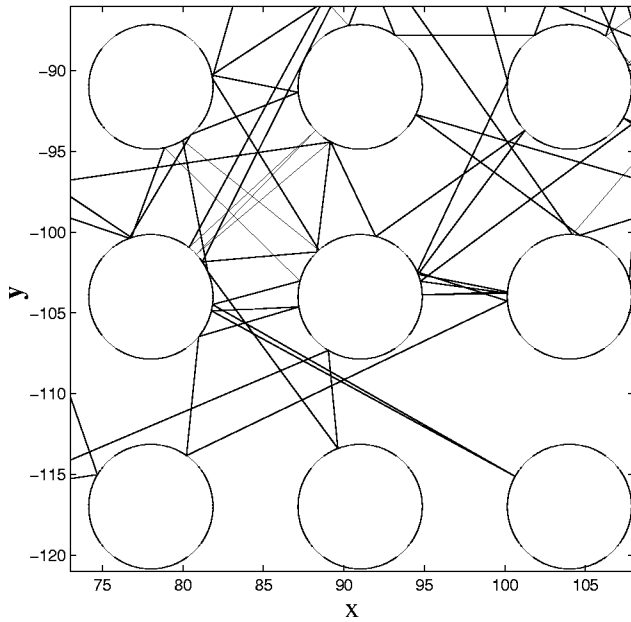


FIG. 5. A particle trajectory in the Lorentz gas.

Let  $N(l, t; \varepsilon, \varepsilon_0)$  be the non-normalized complexity function introduced in Eqs. (7) and (31) and, for simplicity, use the notation  $N(l, t)$  omitting  $\varepsilon, \varepsilon_0$ . A silent assumption is that for fairly small  $\varepsilon_0, \varepsilon$  and fairly large  $\varepsilon/\varepsilon_0$  and  $N$  the result for  $N(l, t)$  has a stable limit. Consider two projections

$$N(|y|) = \int_0^\infty dt' N(|y|, t'),$$

$$N(t) = \int_0^\infty d|y|' N(|y|', t), \quad (38)$$

where we replaced  $l \rightarrow y$  due to the one-dimensionality of the diffusion process. It is convenient to introduce also the numbers of all separated pairs by time  $t$ :

$$N_t(|y|) = \int_0^t dt' N(|y|, t') \quad (39)$$

with the evident relation

$$N_\infty(|y|) = N(|y|), \quad t \rightarrow \infty. \quad (40)$$

It is supposed in Eqs. (37)–(40) that the distribution  $F(y, t)$  is symmetric:  $F(y, t) = F(-y, t), t \rightarrow \infty$ .

The main results of the simulation are shown in Figs. 9–11. They can be interpreted in the following way.

*Conjecture 2.* For the bar billiard

$$\mu_r = \mu \quad (41)$$

in Eqs. (17) and (18), i.e.,

$$N_t(|y|) = (\text{const}) \times |y|^\delta \Phi(\xi), \quad t \rightarrow \infty, \quad (42)$$

with some  $\delta$  and

$$\xi = |y|/t^{\mu/2}. \quad (43)$$

In Fig. 9 self-similar front propagation is evident, and the numbers give  $\mu = 1.82$  in good agreement with the value of  $\mu = 1.75$ . The value  $\delta \approx -2.86$ , which is close to  $-2.7$  in Fig. 10, is in agreement with Eq. (42).

Figure 11 needs a more sophisticated analysis. In correspondence to Conjecture 1 and definition (21),

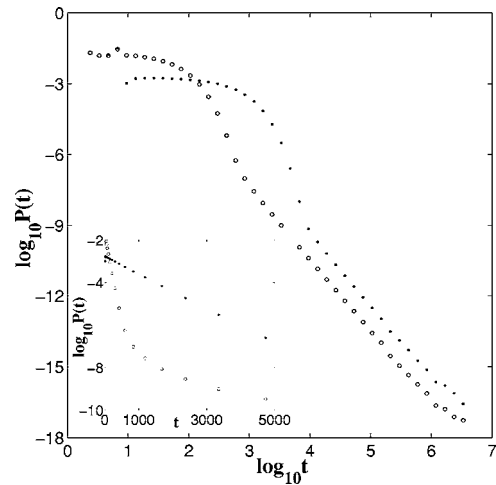


FIG. 6. Probability density of recurrences after time  $t, P(t)$ , for the Sinai billiard: a circle of radius  $r = 0.55944106$  in a  $2 \times 2$  box ( $-1 < x < 1, -1 < y < 1$ ). 1536 initial conditions; run time is  $10^{10}$  for each trajectory (velocity is 1). Dots: returns to  $x = 1, 0 < y < 0.2, 0.55 < v_y < 0.75$ . log-log slope is  $-3.029$  for  $4.125 < \log_{10} t < 5.925$ ; semilog slope is  $-0.0008$  for  $26 < t < 5000$ ; Circles: returns to  $x = 1, 0 < y < 0.2, -1 < v_y < 1$ . The log-log slope is  $-3.013$  for  $3.225 < \log_{10} t < 5.925$ ; the semilog slope is  $-0.0078$  for  $9 < t < 600$ .

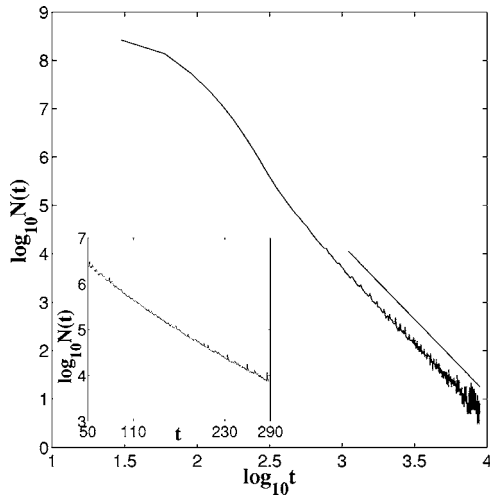


FIG. 7. Number of pairs  $N(t)$  separated for the first time at  $t$  for the Sinai billiard: a circle of radius  $r=3.862\,581\,7$  in a  $13 \times 13$  box. One trajectory runs for time  $3 \times 10^{10}$ . Initial separation is  $\varepsilon_0 = 0.0001$  along the lower side of the square;  $\varepsilon = 0.01$ .

$$N(t) = (\text{const}) \times P(t) = (\text{const})/t^\gamma. \quad (44)$$

Following Eqs. (38) and (44), we have

$$P(t)dt = dt \int_0^\infty \rho(y,t)dy = (\text{const}) \times dt \int_0^\infty N(y,t)dy = (\text{const}) \times dt t^{\mu/2} \Phi(t) \quad (45)$$

where

$$\Phi(t) = \int_0^\infty \rho(\xi,t)d\xi = \frac{(\text{const})}{t^{\delta_1}}. \quad (46)$$

From  $N(t) = (\text{const}) \times \Phi(t)$  and Fig. 11 we have  $\delta_1 = 3.4$ . From the other side,

$$\Phi(t)dt = (\text{const}) \times t^{\delta_1} \frac{dt}{da} da \quad (47)$$

where we consider ensemble  $a_n$  and

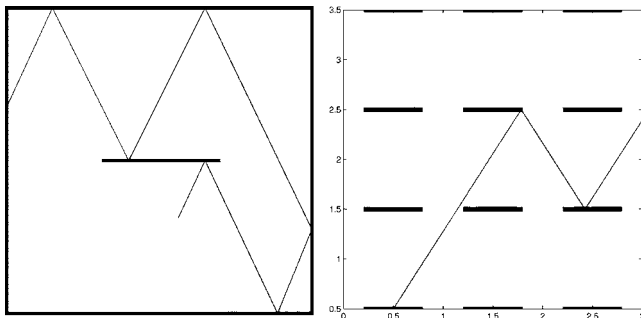


FIG. 8. An example of a trajectory in a bar-in-square billiard and its periodically continued form. On the left is a unit square, on the right is a part of the infinitely continued left billiard. The coordinates are the same as in Fig. 5.

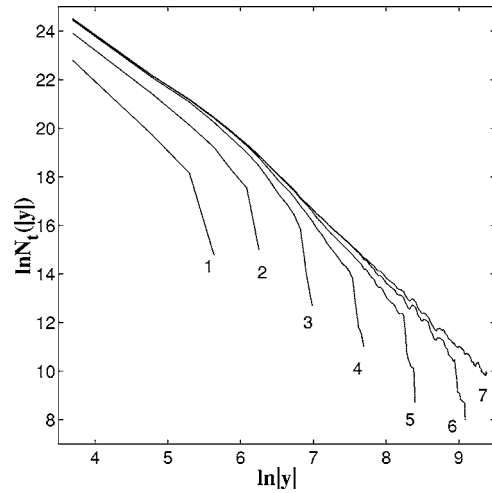


FIG. 9. Bar-in-square billiard with the base cell  $1 \times 1$  and the bar length  $c=0.411\,017$ .  $N_i(|y|)$  distribution for separation of two trajectories by time  $t_n$ .  $N=5.2 \times 10^{10}$  pairs of trajectories. Angular separation in a pair  $\varepsilon_0=10^{-6}$  and  $\varepsilon \sim 1$ . Angles  $\vartheta=0.9+10^{-11}i$  for  $0 < i < 5.24 \times 10^{10}$ ;  $t_n=420 \times 2^n$  for  $n=0,1,2,3,4,5,6$  (from the left to the right, curves 1–7). For  $\ln|y| > 7$  the slope is  $-2.86$ .

$$\tan \vartheta = a_0 + 1/1 + a_1/1 + \dots = a_0 + [a_1, a_2, \dots] \quad (48)$$

is a representation of the continued fraction. Such an ensemble was introduced in [6] for irrational trajectories and  $[a_1, \dots, a_n]$  is the  $n$ th rational approximant to (48). Then one can write

$$\frac{dt}{da} = \frac{dT_n}{da_n}, \quad n \rightarrow \infty, \quad (49)$$

with

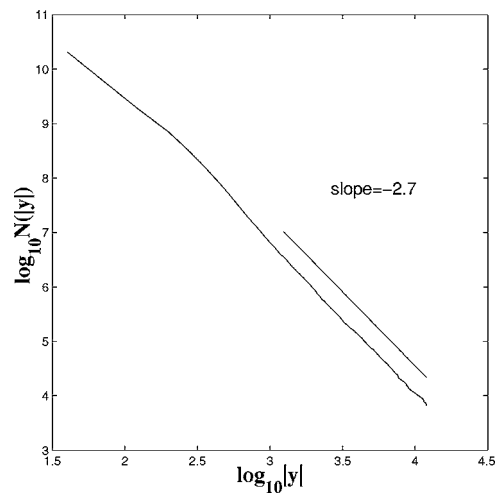


FIG. 10. Bar-in-square billiard with the base cell  $1 \times 1$  and the bar length  $c=0.411\,017$ .  $N_\infty(|y|)=N(|y|)$  distribution for separation of two trajectories.  $5.2 \times 10^{10}$  pairs of trajectories. Angular separation in a pair  $\varepsilon_0=10^{-6}$  and  $\varepsilon \sim 1$ . Angles  $\vartheta=0.9+10^{-11}i$  for  $0 < i < 5.24 \times 10^{10}$ .



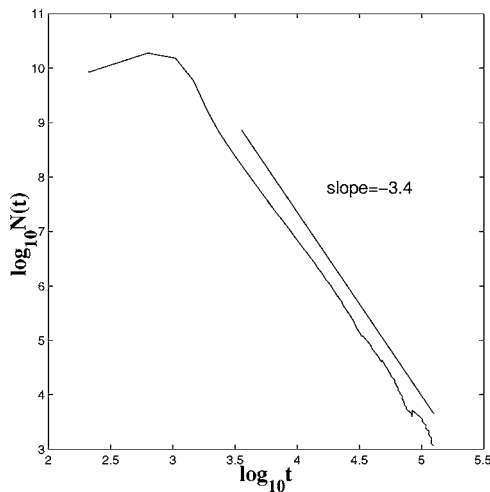


FIG. 11. Bar-in-square billiard with the base cell  $1 \times 1$  and the bar length  $c=0.411\ 017$ . Time distribution for separation of two trajectories.  $5.2 \times 10^{10}$  pairs of trajectories. Angular separation in a pair  $\varepsilon_0=10^{-6}$  and  $\varepsilon \sim 1$ . Angles  $\vartheta=0.9+10^{-11}i$  for  $0 < i < 5.24 \times 10^{10}$ .

$$T_n = \lambda_T^n g_T(n), \quad a_n = \lambda_a^n g_a(n), \quad (50)$$

where the slowly varying functions of  $n$  and the scaling constants are [6,7]

$$\ln \lambda_T = 1.186\dots, \quad \ln \lambda_a = 0.95\dots \quad (51)$$

Applying Eqs. (50) and (51) to Eq. (49) we obtain

$$\frac{dt}{da} = 1/t^{(\ln \lambda_a / \ln \lambda_T - 1)} \quad (52)$$

or

$$P(t)da = (\text{const}) \times dt t^{\mu/2 - 1 + \ln \lambda_a / \ln \lambda_T} \Phi(t). \quad (53)$$

In [6]

$$P(t)da \approx (\text{const}) \times t^\gamma, \quad \gamma = 2.75, \quad (54)$$

was obtained. From Eqs. (51) and (53) we have

$$P(t)da = dt t^{0.87 - 0.2} t^{3.4} = dt t^{2.73} \quad (55)$$

in good agreement with Eq. (54).

### VII. CONCLUSION

In this paper we have discussed some applications of the complexity function introduced in [2]. The complexity function  $\rho$  is a convenient measure that characterizes local insta-

bility properties of dynamical systems, i.e., dispersion of pairs of initially close trajectories. It seems evident that, knowing such a function, one has many possibilities for expressing macroscopic observables through different moments of  $\rho$ .

It was shown in the paper that different properties of particle transport can be described using the distribution of the finite time  $\varepsilon$ -separation of pairs of trajectories for small  $\varepsilon$ . The results were applied to dynamical systems with chaotic and pseudochaotic behavior.

It seems to us that a similar approach can be applied to passive particles moving in turbulent media. The trajectory separation in the velocity space is defined as

$$\delta \mathbf{v}(\mathbf{r}_0, t; \boldsymbol{\varepsilon}, \boldsymbol{\varepsilon}_0) = \mathbf{v}(\mathbf{r}_0 + \mathbf{l} + \boldsymbol{\varepsilon}, t; \mathbf{r}_0 + \boldsymbol{\varepsilon}_0) - \mathbf{v}(\mathbf{r}_0 + \mathbf{l}, t; \mathbf{r}_0). \quad (56)$$

Then we can introduce the CF  $\rho(\mathbf{l}, t; \boldsymbol{\varepsilon}, \boldsymbol{\varepsilon}_0)$ , where  $\boldsymbol{\varepsilon}_0 = \delta \mathbf{r}$  is the initial distance in the coordinate space between trajectories, and consider the structure function

$$\begin{aligned} & \langle |\mathbf{v}(\mathbf{r}_0 + \mathbf{l} + \boldsymbol{\varepsilon}, t; \mathbf{r}_0 + \boldsymbol{\varepsilon}) - \mathbf{v}(\mathbf{r}_0 + \mathbf{l}, t; \mathbf{r}_0 + \boldsymbol{\varepsilon}_0)|^q \rangle \\ &= \langle |\delta \mathbf{v}(\mathbf{r}_0, t; \boldsymbol{\varepsilon}_0, \boldsymbol{\varepsilon})|^q \rangle = \int_0^\infty d\mathbf{r}_0 \rho(\mathbf{r}_0, t; \boldsymbol{\varepsilon}, \boldsymbol{\varepsilon}_0) |\delta \mathbf{v}(\mathbf{r}_0, t; \boldsymbol{\varepsilon}_0, \boldsymbol{\varepsilon})|^q \end{aligned} \quad (57)$$

where we replace the integration over  $\mathbf{l}$  by integration over initial coordinates of particles, i.e., over the particle ensemble. Definition of the structure function can be found in [22,8]. Initially, the pair of trajectories is at  $\mathbf{r}_0$  and  $\mathbf{r}_0 + \boldsymbol{\varepsilon}_0$ . At time  $t$  the particles are at  $\mathbf{r}$  and  $\mathbf{r} + \mathbf{l}$ , correspondingly, i.e.,  $\mathbf{l}$  is the pair separation at time  $t$ . In turbulence theory and experiment [23,24] we are interested in the dependence

$$\langle |\delta \mathbf{v}(\mathbf{r}_0, t; \boldsymbol{\varepsilon}_0, \boldsymbol{\varepsilon})|^q \rangle \sim \varepsilon^{\mu_l(q)} \quad (l \gg \varepsilon \gg \varepsilon_0) \quad (58)$$

related to the so-called Richardson law. The relation between Lévy walks and the Richardson law was pointed out in [25]. With the help of the complexity function  $\rho$ , we are connecting some specific features of the dynamics to the macroscopic observables. This connection will be discussed in more detail elsewhere.

### ACKNOWLEDGMENTS

This work was supported by the Office of Naval Research, Grant No. N00014-02-1-0056, the U.S. Department of Energy Grant No. DE-FG02-92ER54184, and the NSF Grant No. DMS-0417800 Simulation was supported by NERSC.

[1] G. M. Zaslavsky, Phys. Rep. **371**, 461 (2002).  
 [2] V. Afraimovich and G. M. Zaslavsky, Chaos **13**, 519 (2003).  
 [3] C. E. Shannon, in *Information and Decision Processes*, edited by R. Machol (McGraw-Hill, New York, 1960), p. 93.  
 [4] A. N. Kolmogorov and V. M. Tikhomirov, Usp. Mat. Nauk,

**14**, 3 (1959).  
 [5] R. Bowen, Trans. Am. Math. Soc. **84**, 125 (1973).  
 [6] G. M. Zaslavsky and M. Edelman, Chaos **11**, 295 (2001).  
 [7] G. M. Zaslavsky and M. Edelman, in *Perspectives and Problems in Nonlinear Science*, edited by E. Kaplan, J. E. Marsden,

- and K. R. Sreenivasan (Springer, New York, 2003), p. 421.
- [8] T. Bohr, M. H. Jensen, G. Paladin, and A. Vulpiani, *Dynamical Systems Approach to Turbulence* (Cambridge University Press, Cambridge, U.K., 1998).
- [9] E. Ott, *Chaos in Dynamical Systems* (Cambridge University Press, Cambridge, U.K., 1993).
- [10] X. Leoncini and G. M. Zaslavsky, Phys. Rev. E **65**, 046216 (2002).
- [11] G. M. Zaslavsky, *Hamiltonian Chaos and Fractional Dynamics* (Oxford University Press, Oxford, 2005).
- [12] J. D. Meiss, Chaos **7**, 39 (1997).
- [13] A. Katok and B. Hasselblatt, *Introduction to the Modern Theory of Dynamical Systems* (Cambridge University Press, Cambridge, U.K., 1995).
- [14] G. A. Margulis, Funkc. Anal. Priloz. **3**, 80 (1969); **4**, 62 (1970).
- [15] H. Bruin, B. Saussol, S. Troubetzkoy, and S. Vaienti, Ergod. Theory Dyn. Syst. **23**, 991 (2003).
- [16] G. M. Zaslavsky, Physica D **76**, 110 (1994).
- [17] G. M. Zaslavsky, M. Edelman, and B. A. Niyazov, Chaos **7**, 159 (1997).
- [18] S. Benkadda, S. Kassibrakis, R. B. White, and G. M. Zaslavsky, Phys. Rev. E **55**, 4909 (1997).
- [19] R. B. White, S. Benkadda, S. Kassibrakis, and G. M. Zaslavsky, Chaos **8**, 757 (1998).
- [20] L. A. Bunimovich and Ya. G. Sinai, Math. USSR. Sb. **90**, 407 (1973); L. A. Bunimovich, Commun. Math. Phys. **65**, 295 (1979).
- [21] E. Gutkin, Physica D **19**, 311 (1986); J. Stat. Phys. **83**, 7 (1996).
- [22] U. Frisch, *Turbulence: The Legacy of A. N. Kolmogorov* (Cambridge University Press, Cambridge, U.K., 1995).
- [23] M. C. Jullien, P. Castiglione, and P. Tabeling, Phys. Rev. E **64**, 035301(R) (2001).
- [24] M. C. Jullien, J. Paret, and P. Tabeling, Phys. Rev. Lett. **82**, 2872 (1998).
- [25] M. F. Shlesinger, B. J. West, J. Klafter, Phys. Rev. Lett. **58**, 1100 (1987).